JOURNAL OF AGRICULTURAL AND FOOD CHEMISTRY
ARTICLE

J. Agric. Food Chem. 2009, 57, 7377–7386 7377
DOI:10.1021/jf9012423

Isothermal and Non-isothermal Kinetic Models of Chemical Processes in Foods Governed by Competing Mechanisms

Micha Peleg,*,† Maria G. Corradini,§ and Mark D. Normand†

†Department of Food Science, University of Massachusetts, Amherst, Massachusetts 01003, and §Instituto de Tecnología, Facultad de Ingeniería y Ciencias Exactas, Universidad Argentina de la Empresa, Cdad. de Buenos Aires, Argentina

A process or reaction that peaks at high temperatures but not at low ones indicates competition between synthesis and degradation. A proposed phenomenological model composed of a decay factor superimposed on a growth term can describe both. Temperature elevation shortens the two subprocesses' characteristic times and increases their rates. The degradation's characteristic time relative to the experiment's determines whether a peak is observed. All of the parameters determine the peak's height and shape as can be seen in two interactive Wolfram demonstrations on the Web. Detailed knowledge of the underlying mechanisms is unnecessary for the model's construction, and uniqueness is not a prerequisite either. However, different expressions might be needed for ongoing processes and ones initially undetectable. The model's applicability is demonstrated with published results on very different reactions in foods. In principle, it can be converted into a dynamic rate equation for simulating a process's evolution under non-isothermal conditions.

KEYWORDS: Competing reactions; peak concentration; kinetics; lipid oxidation; acrylamide; growth and mortality; Wolfram Demonstration Project

INTRODUCTION

The kinetics of chemical reactions and biochemical or biological processes has been primarily studied in systems in which the reactants' and products' concentrations decrease or increase monotonically. Food examples are the thermal degradation of vitamins or the accumulation of enzymatic reaction products (*1*). Certain chemical processes, however, are characterized by a notable peak product concentration, at (relatively) high temperatures but not at low. Examples are acrylamide in baked or fried foods (*2*−*4*) and lipid oxidation monitored by the peroxide value rise (*5*−*8*). The dynamics of such processes has been traditionally studied by following a set of several intermediate reactions. The simplest is when a compound B is the product of a reaction of the general type A → B → C, in which case a peak in its concentration can be observed depending on the synthesis and degradation reaction rates (*1*). In most published studies of complex processes of this kind, it has been assumed that all of the intermediate reactions follow first- or other fixed-order kinetics and that the temperature dependence of their rate constants obeys the Arrhenius equation (*9*, *10*). This entails that each intermediate reaction has a temperature-independent "energy of activation", unaffected by the changing chemical and/or physical environment. The merits and limitations of this approach have been discussed elsewhere (*1*, *11*−*13*). Suffice it to say here that identification and monitoring of all the intermediate reactions and their kinetics may require sophisticated analytical methods such as NMR, HPLC, and calorimetry, which can become a logistic constraint. Therefore, a mathematical model or models that could describe and predict a process's kinetics on the basis of its final product's concentration alone would have obvious practical advantages. The above statement should not be construed as a suggestion that the mechanistic approach should not be pursued. On the contrary, insight into a process's mechanism and its kinetics is and will remain essential to its control by chemical means. A discussion and examples of "peaked reactions" in foods can be found in van Boekel's comprehensive new book on the kinetics of food systems (*1*). The rise and fall of blood glucose after a meal is another example of a "peaked process" (*14*, *15*) and so is that of the corresponding insulin level. A rise and fall pattern can also be observed during the administration of antibiotics and other drugs (*16*), as well in the histamine production triggered by an allergen [see, e.g., Baroody et al. (*17*)]. [Even microbial growth and mortality in a closed habitat can be viewed as a peaked process, despite the fact that its "reactants" are cells rather than molecules [see, e.g., Dougherty et al. (*18*)].] The same can be said about the growth of certain tissue cultures [see, e.g., Liu et al. (*19*) and Sitton and Srienc (*20*)].

Common to all these peaked reactions and processes is dynamics controlled by competing mechanisms that operate *simultaneously*; one promotes synthesis, generation, or growth, the other, degradation, disintegration, or, in the case of cells, death. A complete account of the elements involved in a complex multistage process, and of their interactions, is frequently lacking. Moreover, it is uncertain that exactly the same mechanisms operate at different temperatures, as is commonly assumed. Actually, because of the continuously varying chemical and physical environment in foods, there is good reason to suspect that a temperature change might affect different elements of the process in different ways. For example, the "limiting reaction" at

*Corresponding author [telephone (413) 545-5852; fax (413) 545-1262; e-mail micha.peleg@foodsci.umass.edu].

Published on Web 07/28/2009

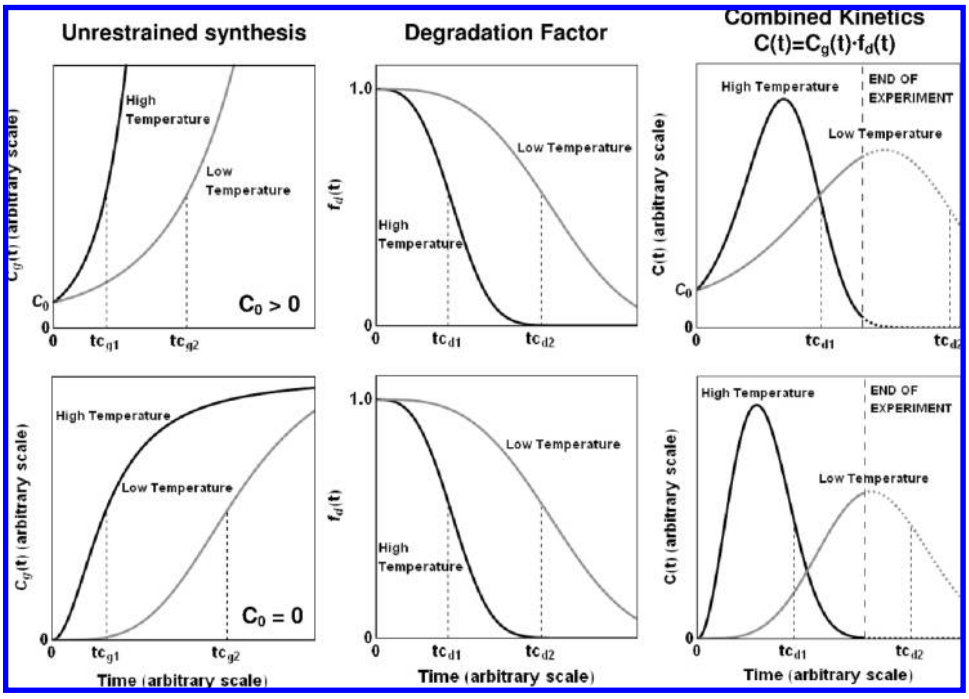

Figure 1. Schematic view of the isothermal model construction: (top) for systems with a nonzero initial product concentration; (bottom) for systems with zero initial product concentration. Note that a peak concentration is only observed when the degradation's characteristic time constant, t_{cd}, falls within or close to the experiment's duration. Also notice that a temperature rise shortens the two characteristic times and increases the steepness of the curve's rise and fall.

a given temperature might not be the same at a higher or lower temperature. Theoretically, at least, as the chemical environment is altered, interactions or pathways can be fully or partially opened or blocked. Let us therefore deal with the phenomenology of peaked processes' kinetics. The starting point is the admission that the details are unknown or might be even unknowable. We can say, though, that an isothermal peaked process can be described mathematically by a global growth term on which a decay factor has been superimposed, as shown schematically in **Figure 1**. The first term, the "growth component" of the model (left) represents a hypothetical unrestrained synthesis. It would have taken place had there been no degradation and physical constraints on the system. The second term, the "decay factor" (middle), represents the total effect of the degradation mechanisms. The superposition of the two produces the actually observed concentration curve (right). Note that the unrestrained growth or generation curve, $C_g(t)$, and the decay or degradation factor, $f_d(t)$, have different temperature-dependent characteristic times (t_{cg1} or t_{cg2} vs t_{cd1} or t_{cd2} as shown in the figure). Thus, when t_{cd} falls within or close to the experiment's time, a peak concentration will always be observed, but if t_{cd} is well beyond the experiment's duration, the concentration versus time curves will appear to be monotonically rising. The curve's concavity direction in this case will be determined by that of $C_g(t)$. When a peak concentration does appear, its shape will depend on the process's characteristics, represented by $C_g(t)$ and $f_d(t)$; that is, its height, width, and degree of symmetry will vary with temperature in a manner dictated by the temperature dependence of these two functions' coefficients.

Figure 1 depicts two scenarios: where the curve starts at a nonzero initial concentration (top) and where it starts from zero (bottom). The reason for and implications of the distinction are discussed in the following section. The above modeling approach has already been applied to lipid oxidation (*21*) and acrylamide formation and degradation (*22*), albeit with slightly different mathematical expressions. They have been replaced for the present work to develop a dynamic rate model for simulating non-isothermal peaked processes that is consistent with physical considerations.

METHODS: MODEL DEVELOPMENT

Isothermal Generation and Degradation. *Starting from a Finite Initial Concentration*. Consider a reaction or process whereby the initial product's concentration is $C_0 > 0$. An example is oil oxidation starting with a measurable peroxide value. If the synthesis or growth process could proceed uninterrupted, the product's concentration would increase indefinitely (which is impossible, of course, for mass balance considerations). A convenient flexible model that can describe such unrestrained rise is the stretched exponential expression

$$C_g(t) = C_0 \exp\left(\frac{t}{t_{cg}}\right)^{m_1} \quad m_1 > 0 \tag{1}$$

where C_0 is the initial concentration in the pertinent units, t_{cg} a characteristic time, and m_1 a power representing the curve's steepness. [In what follows we will only refer to chemical processes and hence use concentration terms. It is self-evident that $C_g(t)$ and C_0 can be replaced by $N_g(t)$ and N_0 when the growth of living cells is concerned.] According to this model when $t = t_{cg}$, $C_g(t) = C_0 \exp(1) = 2.718\ C_0$, regardless of the magnitude of m_1. Also note that $m_1 > 1$ implies that $C_g(t)$ has upper concavity and $m_1 < 1$ downward concavity. $m_1 = 1$ is a special case where $C_g(t)$ rises linearly.

Exponential growth, as already mentioned, cannot be sustained indefinitely, in our case because there is a finite supply of reactants. Consequently, the product's concentration must either approach an asymptotic value or, if it is chemically degraded, its concentration at some point will decline. The existence of degradation, which might commence while the product's total concentration is still rising, can be represented by a degradation factor, $f_d(t)$. Its range if the product tends to disappear completely will be from zero to one.

A convenient and flexible mathematical expression that can describe such a decay factor is the stretched exponential

$$f_d(t) = \exp\left[-\left(\frac{t}{t_{cd}}\right)^{m_2}\right] \quad m_2 > m_1 \tag{2}$$

where t_{cd} is the degradation process's characteristic time, that is, at $t = t_{cd}$, $f_d(t) = 1/e = 0.3678$ ..., and m_2 is a parameter representing the decline's steepness.

Combining eqs 1 and 2 yields the generation/degradation model

$$C(t) = C_g(t) f_d(t) \tag{3}$$

or

$$C(t) = C_0 \exp\left(\frac{t}{t_{cg}}\right)^{m_1} \exp\left[-\left(\frac{t}{t_{cd}}\right)^{m_2}\right] \tag{4}$$

Generation Reactions Starting from Zero Product Concentration. Consider a reaction having product(s) that are detectable only beyond a certain temperature. The already mentioned acrylamide formation in foods exposed to high temperatures is a case in point. It is not present in raw potatoes or wheat dough but can be found in French fries and baked breads' crust. In terms of the model, this means that the acrylamide's concentration at time zero is zero. Note, however, that if $C_0 = 0$ is inserted into eq 4, the result will be $C(t) = 0$ for all times, regardless of the other parameters' magnitudes. To avoid this problem, we will redefine the synthesis component of the model. For example, we can assume that $C_g(t)$ is a sigmoid curve described by the empirical model

$$C_g(t) = \frac{C_{asymp}\left(\frac{t}{t_{cg}}\right)^{m_1}}{1+\left(\frac{t}{t_{cg}}\right)^{m_1}} \quad m_1 > 0 \tag{5}$$

where C_{asymp} is a hypothetical concentration level that would have been reached asymptotically had the generation process/synthesis been allowed to proceed uninterrupted, but limited by the amount of available reactants, for example. As before, t_{cg} is the generation process's characteristic time, but here when $t = t_{cg}$, $C_g(t) = C_{asymp}/2$. As before, the parameter m_1 controls the curve's concavity direction and steepness. According to eq 5 at $t = 0$, $C_g(t) = 0$ and at $t \rightarrow \infty$, $C_g(t) \rightarrow C_{asymp}$. The choice of t_{cg} and m_1 offers great flexibility in setting the growth level and the time of its inception. Combining eq 5 with the degradation factor $f_d(t)$ as defined by eq 2 yields the model

$$C(t) = C_{asymp} \frac{\left(\frac{t}{t_{cg}}\right)^{m_1}}{1+\left(\frac{t}{t_{cg}}\right)^{m_1}} \exp\left[-\left(\frac{t}{t_{cg}}\right)^{m_2}\right] \tag{6}$$

All of the previous statements about the roles of t_{cg}, t_{cd}, m_2, and m_1 are valid here, too, with two exceptions: (i) Although eq 6 allows (hypothetical) scenarios of unrestrained growth, that is, if $t_{cd} \rightarrow \infty$ and $C_{asymp} \rightarrow \infty$, it cannot account for a pure decay curve because at $t = 0$, $C(t) = 0$. (ii) Because the first (growth) term has an asymptote, the condition that m_2 must be bigger than m_1 (eq 2) no longer applies.

Non-isothermal Peaking Kinetics. Most of the published works on non-isothermal processes and reactions kinetics deal with systems that under isothermal conditions exhibit a monotonic concentration rise or fall. Vitamin degradation during thermal processing or storage and nonenzymatic browning are typical examples. The issue has been how to use isothermal concentration−time data in the derivation of a model that could predict the decay or growth pattern under non-isothermal conditions. When the reaction or process follow fixed-order kinetics and its rate constant's temperature dependence, the Arrhenius equation, the constant temperature, T, in the rate version of the model has been replaced by a varying temperature term, $T(t)$. Once done, the dynamic concentration curve has been calculated by numerical integration. In cases when the "rate constant" is a function of not only temperature but also time, this method cannot be used. Unlike in classic kinetics, where one deals with a single temperature-dependent rate constant, or two in the case of an A → B → C type peaking reaction, a reaction such as lipid oxidation is characterized by at least four temperature-dependent parameters, namely $t_{cg}[T]$, $m_1[T]$, $t_{cd}[T]$, and $m_2[T]$, according to eq 4, and acrylamide formation by at least five according to eq 6, if $C_{asymp}[T]$ is not constant. Also, in the absence of a theory to derive these parameters from first principles, their temperature dependence ought to be described by two- or three-parameter ad hoc empirical expressions, which complicates the rate model even further. Thus, to predict correctly a peaked process's non-isothermal evolution, one has to derive a four- or five-parameter expression having coefficients that are not constants but functions of the changing temperature and hence of time. Examples of this modeling approach in microbial inactivation and growth can be found in Peleg and Penchina (*23*) and Corradini and Peleg (*24*) and in vitamin loss in Corradini and Peleg (*25*). The underlying assumption in these works was that under dynamic conditions, the momentary ("instantaneous") logarithmic decay or growth rate, in our case $d\log[C(t)/C_0]/dt$, is the isothermal logarithmic rate at the momentary temperature, $T(t)$, at a time, t^*, that corresponds to the momentary concentration ratio, that is, to the system's momentary state. The applicability of the concept, which applies only to systems where $C_0 > 0$, has been confirmed by the ability of the resulting rate models to predict correctly the outcome of non-isothermal heat treatments and storage conditions from isothermal experimental data (*12*, *23*, *24*, *26*). Because the validity of the underlying assumption is not contingent on the use of any particular decay or growth model, any expression that adequately describes the isothermal data will do as a starting point. As demonstrated by Corradini and Peleg, (*24*, *25*) and others, models based on very different mathematical expressions rendered almost indistinguishable correct predictions when derived from the same isothermal database. However, this will be true only if the dynamic models are not used for extrapolation. As long as the rate model is used in the time−temperature range covered by the experimental isothermal data, it does not have to be unique to be predictive.

In principle, the concept of converting algebraic isothermal models into dynamic rate models can be extended to nonmonotonic growth and decay patterns, which include peaked chemical reactions and biological processes. However, before this can be done two issues ought to be addressed: In the pertinent range, except for at the peak itself, every value of $C(t)$ or $\log C(t)$ has *two* corresponding times, not one. Therefore, t^*, which is uniquely defined for a monotonic rise or fall, can now have two values. This problem is avoided when t^* is calculated numerically at successive time intervals starting from zero (see below). The Mathematica program that we have used to solve the rate equation and generate the non-isothermal $C(t)$ curve does it automatically, provided t^* is entered in the appropriate syntax, thus eliminating the ambiguity concerning the curve's ascent and descent. Expressing the rate is the second issue. If we write the rate in terms of the concentration or concentration ratio, instead of its logarithm, the negative slope at the postpeak region can "drag" the solution into negative territory, rendering values that have no physical meaning. Consequently, formulating the rate equation in terms of $d\log C(t)/dt$ is imperative in our case to guarantee a solution that satisfies the condition $C(t) \geq 0$ for any value of t.

Unlike in vitamin degradation or microbial inactivation and growth, for example, published isothermal and dynamic data on the same "peaked" system are extremely rare and might not even exist. Consequently, direct validation of the model by comparing its predictions to actual experimental data has not been an option. All we could do, therefore, was to test the models' internal consistency with computer simulations. Nevertheless, the two models that we propose are both testable in principle, that is, their validity can be confirmed or refuted by comparing their prediction with experimental data. Note that expressing the rate in a logarithmic form in the model equation has no bearing on its parameters' derivation and fit. The data used for these purposes can remain in the form of $C(t)$ or $C(t)/C_0$ versus time relationships and so the model's equations (see below).

Non-isothermal Peaking Kinetics where $C_0 > 0$. Consider a reaction/process for which the isothermal progress follows eq 4 as a model. Converted to a logarithmic relationship it becomes

$$\log C(t) = \log C_0 + \left(\frac{t}{t_{cg}}\right)^{m_1} - \left(\frac{t}{t_{cd}}\right)^{m_2} \quad m_2 > m_1 \tag{7}$$

The momentary logarithmic *climb or descent rate* at time t^*, which corresponds to the momentary concentration, is therefore

$$\frac{d\log C(t)}{dt} = \frac{m_1}{t_{cg}}\left(\frac{t^*}{t_{cg}}\right)^{m_1-1} - \frac{m_2}{t_{cd}}\left(\frac{t^*}{t_{cd}}\right)^{m_2-1} \tag{8}$$

However, because eq 7 has no analytic inverse, the value of t^* must be extracted numerically. In the syntax of Mathematica, the solution of

eq 7 that yields the value of t^* is written in the form

$$t\text{star}[t\_]:= t/x \rightarrow \text{first Nsolve}\left[\left(\frac{x}{t_{cg}[t]}\right)^{m_1[t]}-\left(\frac{x}{t_{cd}[t]}\right)^{m_2[t]}+\log[y\text{init}]==s[t],x\right] \quad (9)$$

[This expression says that the momentary t^* at any real time t, "$t$star[t]", gets the value of the solution of eq 7, where $s[t]$ is log $C(t)$ and $y$init is C_0. The need for the dummy variable x arises because eq 7's coefficients are already functions of the real time t.]

Once defined in this way, $t$star[t] is recognized by the program as a regular function (like log[x] or exp[x], etc.), and its value will be calculated every time the term is called for during the program's execution. With this definition of t^*, eq 8 becomes

$$dLy[t\_]:=\frac{m_1[t]}{t_{cg}[t]}\times\left(\frac{t\text{star}[t]}{t_{cg[t]}}\right)^{m_1[t]-1}-\frac{m_2[t]}{t_{cd}[t]}\times\left(\frac{t\text{star}[t]}{t_{cd}[t]}\right)^{m_2[t]-1} \quad (10)$$

and its solution, "ndresult", is obtained by executing

$$\text{ndresult}=\text{NDSolve}[\{s[t]==dLy[t],s[0]==\log[y\text{init}]\},s[t],[t,0,t\text{cycle}]\} \quad (11)$$

where $t$cycle is the experiment's duration.

In our case, Mathematica's NDSolve[ ] tries to find a function $s(t)$ having a time derivative (the logarithmic curve's momentary slope) $s'[t]$ of $dLy[t]$ as defined by eq 10, that is, where $t$star[t] is calculated anew at every iteration. The boundary condition in this case is that at $t=0$, $s[0]=\log C_0$, $y$init in the Mathematica version of the equation. Because ndresult is not an analytic function, Mathematica returns the solution as an "Interpolation Function", which is a dense set of numerical values, in our case between zero and *tcycle*. Once $s[t]$ is found in this way, it can be converted into a concentration versus time relationship by the substitution

$$C[t]=C_0\exp[\text{ndresult}[[1,1,2]] \quad (12)$$

Having done that, $C[t]$ can be generated and plotted with any C_0 value and chosen $m_1[t]$, $t_{cg}[t]$, $m_2[t]$, and $t_{cd}[t]$ (see below). Despite the cumbersome appearance of the procedure, it is rather simple to those familiar with Mathematica and its syntax. Moreover, once the program has been written, one can define the temperature dependence of the model's coefficients, that is, $m_1[T]$, t_{cg}[T], m_2[T], and t_{cd}[T], in terms of algebraic expressions. Thus, for any given temperature history, $T(t)$, the corresponding rate equation's coefficients are redefined as the nested terms $m_1[t]=m_1[T(t)]$, $t_{cg}[t]=t_{cg}[T(t)]$, $m_2[t]=m_2[T(t)]$, and $t_{cd}[t]=t_{cd}[T(t)]$. These terms, in turn, can be inserted into the rate model's equation, eq 10, the substituted solution of which (eq 12) is the sought concentration versus time curve for the particular temperature history, $T(t)$.

Non-isothermal Peaking Kinetics where $C_0 = 0$. Consider a reaction with isothermal evolution following eq 6 as a model, that is, where the product's initial concentration is zero. The logarithmic rate equation in this case is

$$\log C(t)=\log C_{asymp}+\log\left[\frac{\left(\frac{t}{t_{cg}}\right)^{m_1}}{1+\left(\frac{t}{t_{cg}}\right)^{m_1}}\right]+\left(\frac{t}{t_{cd}}\right)^{m_2} \quad (13)$$

and its rate version is

$$\frac{d\log C(t)}{dt}=\frac{m_1-m_2\left(\frac{t*}{t_{cd}}\right)^{m_2}\left[1+\left(\frac{t*}{t_{cg}}\right)^{m_1}\right]}{t*\left[1+\left(\frac{t*}{t_{cg}}\right)^{m_1}\right]} \quad (14)$$

where t^* is the numerical solution of eq 13 for t (expressed in a manner similar to that of eq 9).

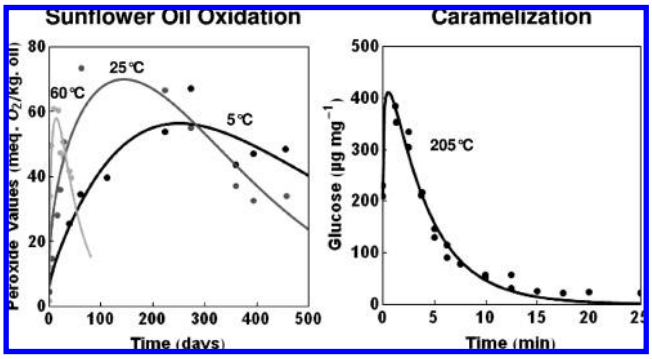

Figure 2. Demonstration of the fit of eq 4 to published peaking concentration data. The experimental results are from Calligaris et al. (*5*) (sunflower oil) and Jiang et al. (*27*) (caramelization, 205 °C).

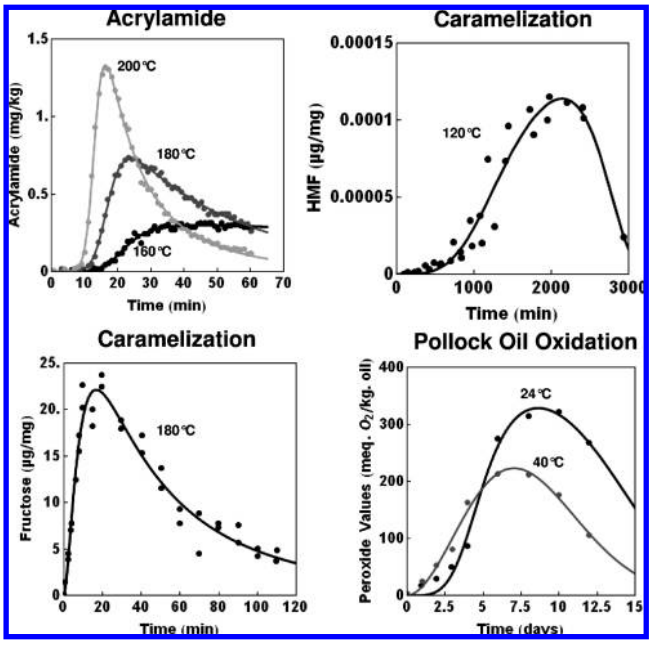

Figure 3. Demonstration of the fit of eq 6 to published peaking concentration data. The experimental results are from Cook and Taylor (*2*) (acrylamide), Jiang et al. (*27*) (caramelization, 180 °C), Quintas et al. (*28*) (caramelization, 120 °C), and Sathivel et al. (*8*) (pollock oil oxidation). The fit parameters of acrylamide are listed in **Table 1**.

Table 1. Acrylamide Formation and Degradation,Regression Parameters of Equation 6 as a Model[a]

temp (°C)	C_{asymp}(mg/kg)	t_{cg} (min)	m_1	t_{cd}(min)	m_2	MSE
160	0.35	22.5	5.9	645	0.73	0.0003
180	2.0	17.7	7.3	26.8	0.82	0.0003
200	4.8	13.1	10.6	13.3	0.95	0.0004

[a] The original data are from Cook and Taylor (*2*). The corresponding plot is shown in **Figure 3**.

The final differential equation, the equivalent of eq 10, written in the syntax of Mathematica is

$$dLy[t\_]:=\frac{m_1[t]-m_2[t]\left(\frac{t\text{star}[t]}{t_{cd}[t]}\right)^{m_2[t]}\left[1+\left(\frac{t\text{star}[t]}{t_{cg}[t]}\right)^{m_1[t]}\right]}{t\text{star}[t]\left[1+\left(\frac{t\text{star}[t]}{t_{cg}[t]}\right)^{m_1[t]}\right]} \quad (15)$$

However, because the concentration curve starts at zero and log[0] = −∞, the initial zero concentration cannot be entered as boundary condition.

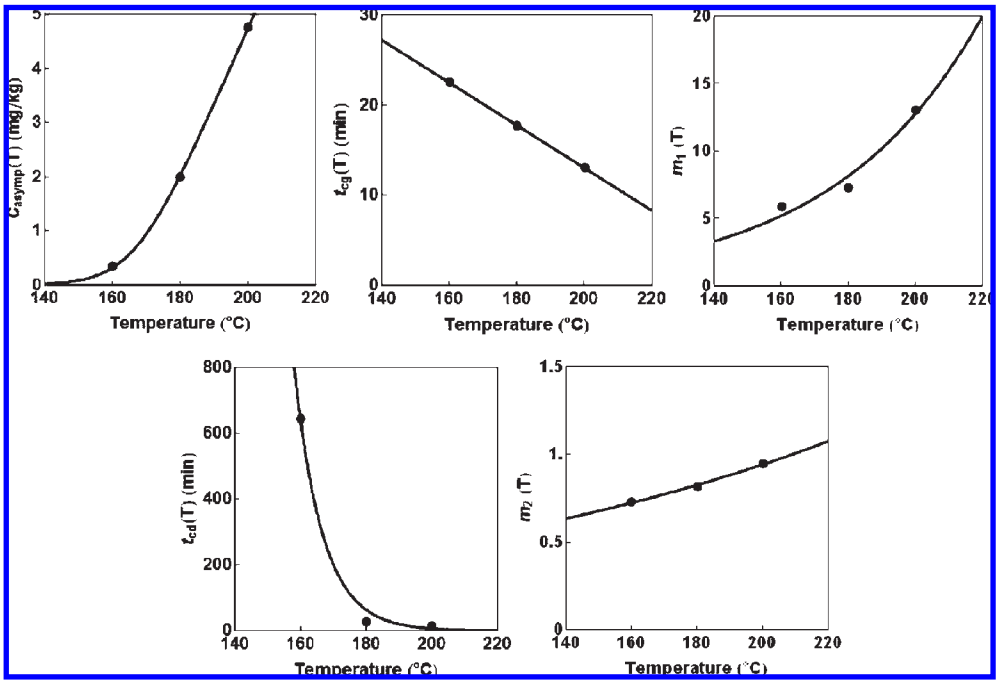

Figure 4. Temperature dependence of the generation and degradation parameters of acrylamide, $C_{asymp}[T]$, $m_1[T]$, $t_{cg}[T]$, $m_2[T]$, and $t_{cd}[T]$ described by ad hoc empirical expressions. The parameters' values were calculated by nonlinear regression from the data shown in **Figure 3** (top left) with eq 6 as a model. The original experimental results are from Cook and Taylor (*2*).

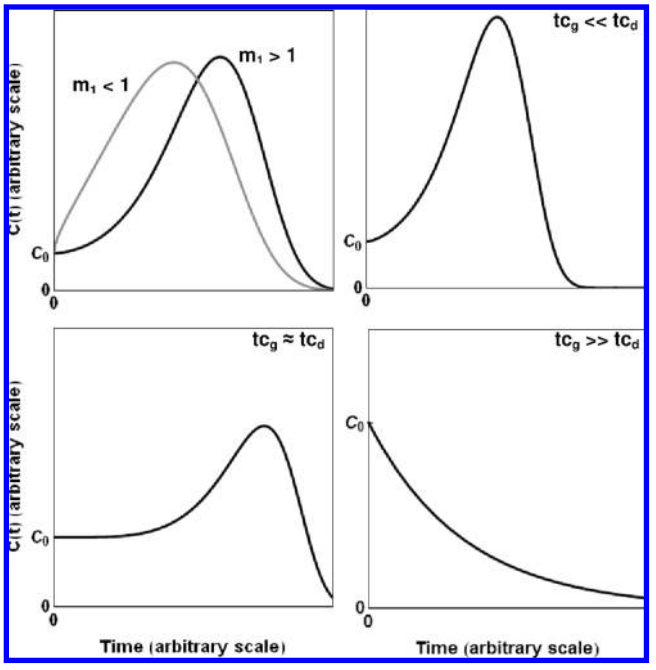

Figure 5. Simulated isothermal peaking concentration curves produced with eq 4 as a model. Note the effect of the generation and degradation parameters on the curves' shape.

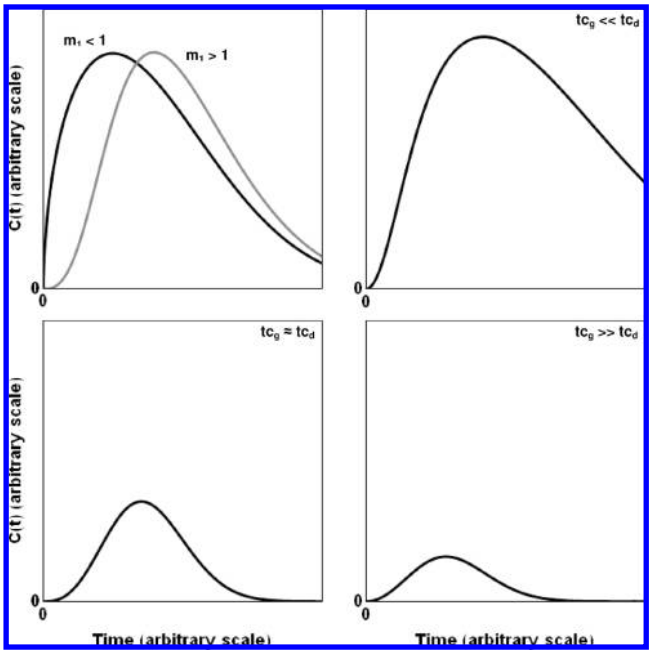

Figure 6. Simulated isothermal peaking concentration curves produced with eq 6 as a model. Note the effect of the generation and degradation parameters on the curves' shape.

The same is true for the curve's tail end where entering an arbitrary very small concentration value for an arbitrary very long time is also not an option. To eliminate the boundary condition problem and come up with a finite value that Mathematica can use, we have to take a detour. Had the synthesis been unimpeded, the isothermal concentration curve would have followed eq 5, which after logarithmic transformation would be written as

$$\log C(t) = \log C_{asymp} + \log\left[\frac{\left(\frac{t}{t_{cg}}\right)^{m_1}}{1+\left(\frac{t}{t_{cg}}\right)^{m_1}}\right] \qquad (16)$$

For non-isothermal conditions, we could derive the logarithmic rate equation in the same manner as before, that is, by assuming that the momentary logarithmic ascent rate is the isothermal logarithmic rate at the momentary temperature, at a time t^* that corresponds to the momentary concentration. In this case, however, the model's equation (eq 5) not only describes a monotonic relationship but it also has an analytic inverse. Consequently, t^* can be extracted and expressed algebraically, that is

$$t*(t) = t_{cg}\left\{\frac{\exp[\log C_g(t) - \log C_{asymp}]}{1-\exp[\log C_g(t) - \log C_{asymp}]}\right\}^{1/m_1(t)} \qquad (17)$$

The non-isothermal differential rate equation of this scenario will therefore be

$$\frac{\mathrm{d}\log C_g(t)}{\mathrm{d}t} = \frac{m_1(t)}{t*(t) + t*(t)\left[\frac{t*(t)}{t_{cg}(t)}\right]^{m_1(t)}} \quad (18)$$

where $t^*(t)$ is defined by eq 17.

Once written in the syntax of Mathematica, eq 18 can be solved numerically by the program. Its coefficients are the hypothetical C_{asymp}, $m_1(t) = m_1[T(t)]$, and $t_{cg}(t) = t_{cg}[T(t)]$, $T(t)$ being the time−temperature relationship or temperature history. The solution of eq 18 is the curve $C_g(t)$ that corresponds to the specified $T(t)$.

Let us now return to the original concentration curve and its description by eq 15. Both curves $C(t)$ and $C_g(t)$ start at zero but later assume very different shapes. However, because at $t \ll t_{cd}$, $f_d(t) \sim 1$, the two curves almost perfectly overlap initially. In other words, unless the two curves diverge very early, any calculated value of $C_g(t)$ at the initial part of the curve will be a close estimate of $C(t)$ at this region and could be used as a boundary condition for the solution of eq 18. To be sure, the solution will not be exact, but it will be very close, so close that curves generated with different values of $C_g(t)$ obtained for different times are practically indistinguishable (see below). Once a boundary condition has been so calculated in this manner, eq 15 can be solved for a variety of temperature histories and the resulting concentration curves examined.

RESULTS AND DISCUSSION

Isothermal Generation and Degradation. The new models' fit has been tested using published results on acrylamide, lipid oxidation, and caramelization reactions. The original data and the fitted concentration curves are shown in **Figures 2** and **3**. The resulting parameters of the acrylamide (which had the lower scatter) are summarized in **Table 1**. The temperature dependence of the generation and degradation parameters can be described by and plotted with ad hoc empirical expressions, as demonstrated with the acrylamide data in **Figure 4**. Data of this kind can be used for quantitative comparison of different synthesis/decay patterns as demonstrated in **Table 1**. They can also be used to identify the temperature level at which the peak concentration will appear, or disappear, and to estimate its height and span at various temperatures, graphically or by calculation.

Simulated generation/degradation curves produced by eq 4 as a model are presented in **Figure 5**. Note that for a peak to appear, m_2 must be larger than m_1. Also, at $t = 0$, $C(t) = C_0$ and as $t \rightarrow \infty$, $C(t) \rightarrow 0$. The time derivative of eq 4 is a cumbersome algebraic expression with no analytical solution for $t > 0$. The peak's location and height, however, can be easily found by using the "FindMax" command of Mathematica (Wolfram Research, Champaign, IL), the program used in this work, or by other numerical methods using alternative software. Equation 4 allows for a scenario whereby $t_{cd} \ll t_{cg}$, in which case $C(t)$ will be a typical exponential decay curve as shown in **Figure 5** (bottom right). Thus, according to the model, monotonic concentration fall,

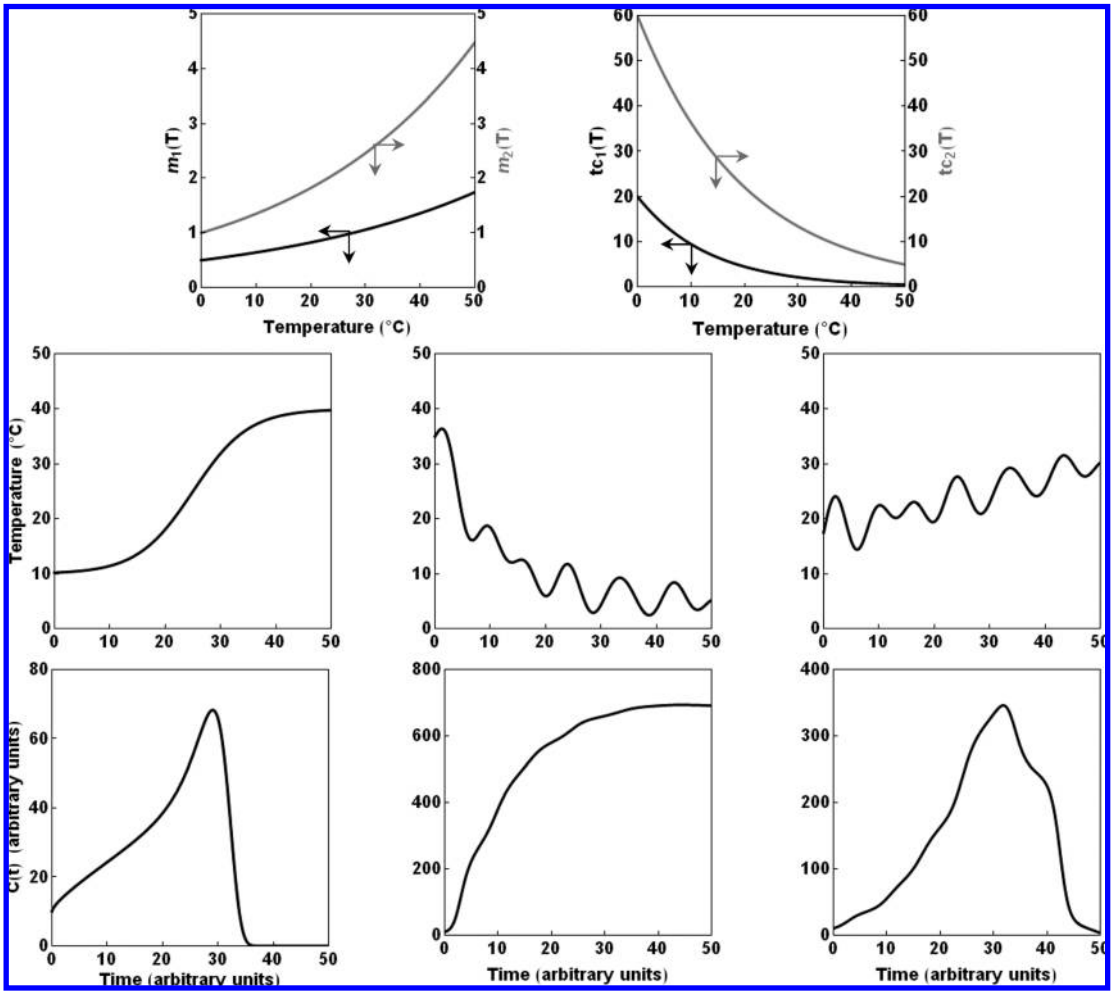

Figure 7. Simulated non-isothermal peaking concentration curves for three temperature histories produced with eq 10 as a model. Note that the rate equation's complexity does not hinder its numerical solution by a program such as Mathematica.

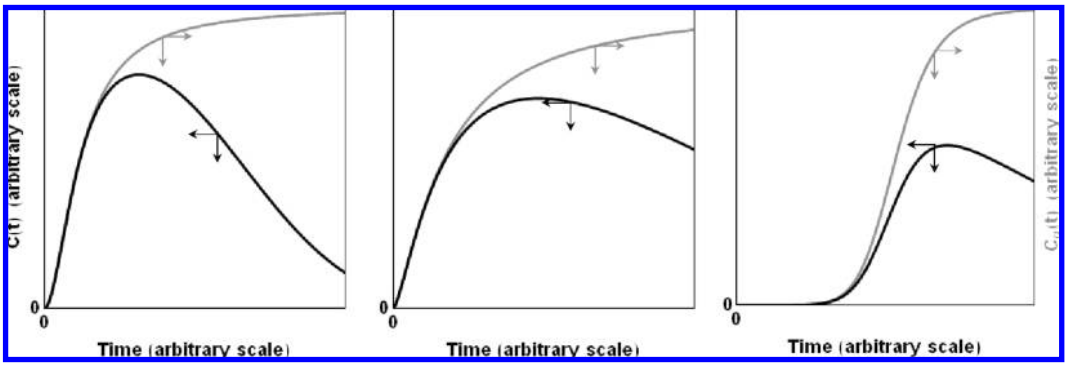

Figure 8. Demonstration of the non-isothermal $C_g(t)$ curve construction with eq 18 as a model to obtain a boundary condition for the solution of eq 14.

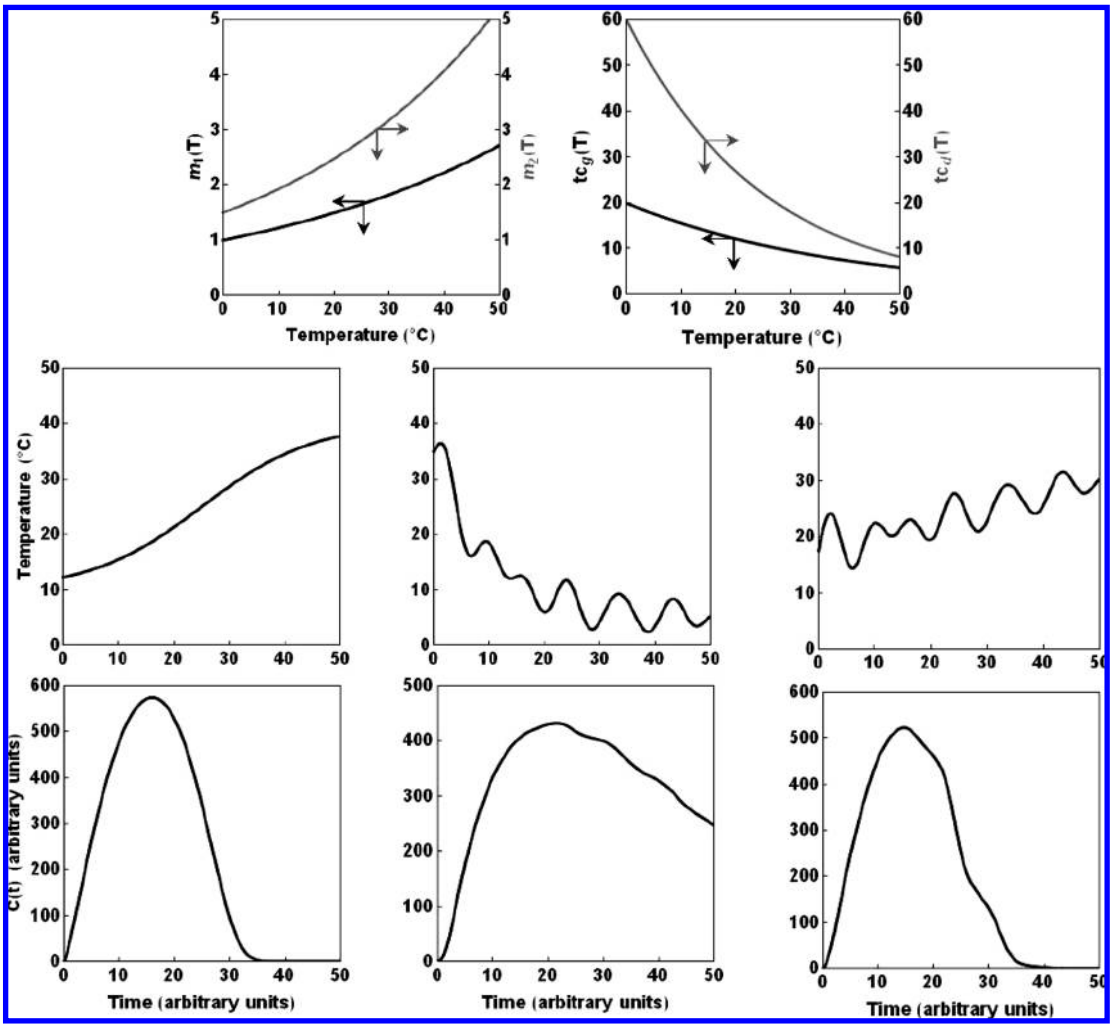

Figure 9. Simulated non-isothermal peaking concentration curves for three temperature histories produced with eq 14 as a model. Note that the rate equation's complexity does not hinder its numerical solution by a program such as Mathematica. Also note that the boundary conditions for the rate equation solution were obtained according to the procedure shown schematically in **Figure 8** and explained in the text.

exponential or logistic, is just a special case of the same kinetics, at least qualitatively.

The model suggests that a smooth transition from predominant synthesis to degradation, or vice versa, is the manifestation of a continuous shift in the characteristic time scales of the underlying processes. The shift can be due solely to the acceleration or retardation of existing reactions, but it can also be caused, at least partly, by extinction of certain reactions and the initiation of new ones. The actual cause can only be determined experimentally by monitoring the intermediate reactions at different temperatures.

Simulated concentration−time relationships produced by eq 6 as a model are shown in **Figure 6**. As could be expected, the peaked curves are similar in appearance to those produced by eq 4, except that they start at zero product concentration. Here too, as shown, one can generate concentration curves with or without a lag time by adjusting the model parameters.

Non-isothermal Generation and Degradation. Examples of a system's dynamic response to different hypothetical temperature histories are given in **Figure 7**. They show peaking kinetics where $C_0 > 0$. The $C(t)$ plots at the bottom were all produced by the

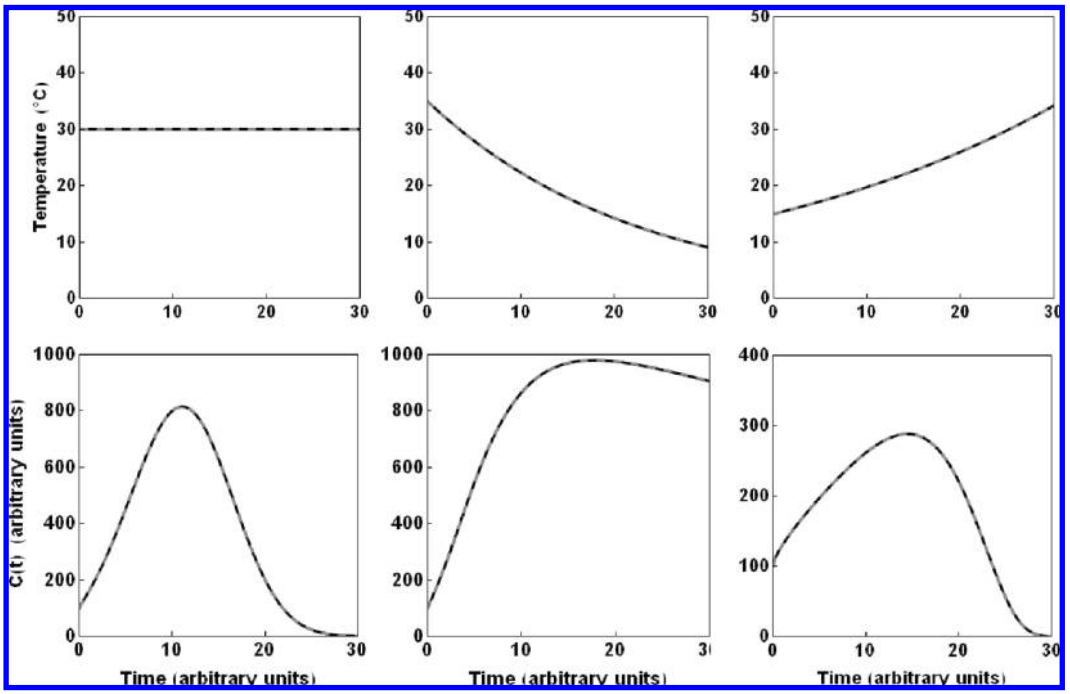

Figure 10. Demonstration of the internal consistency of eq 10 as a rate model. The solid gray and dashed black curves were generated with the temperature profile being described by different algebraic expressions.

described model (eq 10) and procedure. They demonstrate that the mathematical complexity of the rate model's equation, in which all of the coefficients are functions of time, is not a hindrance to its solution by Mathematica. (The solutions were rendered in less than a minute by a computer with a fairly slow processor by today's standards.) Therefore, simulations of the kind shown can be used to examine a variety of scenarios within a very short time.

A similar procedure was used to obtain the dynamic response to the same temperature histories for peaking kinetics when $C_0 = 0$, using eq 14 as the basic model. In this case, however, the boundary condition was first calculated by the method described in the previous section and shown schematically in **Figure 8**. Only then could the rate equation itself be solved to generate the concentration curves shown in **Figure 9**.

Testing the Model's Internal Consistency. The model's consistency and the program's performance were first tested by reproducing known isothermal curves with the non-isothermal version of each model. The isothermal curves were generated with eq 4 and the non-isothermal ones with eqs 7−12. Suppose that for a particular set of $m_1[T]$, $t_{cg}[T]$, $m_2[T]$, and $t_{cd}[T]$ we choose the temperature 30 °C for the isothermal case and insert the corresponding values into eq 4 to produce the concentration curve. We now use the dynamic model for the temperature profile $T(t) = 30 + 10^{-8} \log(t)$, say, or $30-10^{-10}t^{0.3}$. For all practical purposes such "non-isothermal" temperature profiles are identical to the isothermal case when $T = 30$ °C. Therefore, if the non-isothermal model is correct and the calculation method works properly, the curves produced by the two versions of the model should look identical. As demonstrated in **Figure 10** (left) this indeed has been the case. Also, according to the model formulation and its underlying assumption, the mathematical expression that describes the temperature history, $T(t)$, is unimportant, as long as it describes the history adequately. Consequently, if two very different algebraic expressions describe the same temperature profile over the pertinent range, they could be used interchangeably and the resulting concentration curves would be practically indistinguishable. Two examples of this test of the model are given in **Figure 10** (middle and right). The shown concentration curves were produced for what is practically the same temperature profile, except that it was described by a two-parameter exponential term (gray line) and a fourth-degree polynomial (dashed line). As expected, the corresponding concentration curves were also practically identical, and the same has been observed in other simulations of this kind. These included simulations based on eqs 6 and 13−18 as the rate model, that is, for $C_0 = 0$, examples of which are given in **Figure 11**.

All of the above demonstrates that peaking processes can be described by phenomenological models that do not require a priori knowledge of the underlying mechanisms and their kinetics. We repeat that the proposed models are not intended to replace mechanistic ones, only to complement them. The phenomenological models' main advantage is that they can identify the temperature range in which a peak concentration appears or disappears, on the basis of monitoring the final product's concentration alone, a technically simple task in most cases. They also eliminate the need to make assumptions, such as the constancy of the activation energy, which are hard to verify. Because a phenomenological model need not be unique, its choice should be primarily guided by mathematical convenience, the parsimony principle (Occam's razor), and if possible the intuitive meaning of its parameters. Some models, such as the ones discussed in this work, are easier to convert into internally consistent rate equations and can account for the qualitative difference between an ongoing reaction and one starting from a zero initial product concentration ("de novo" synthesis). Future research will show whether the presented dynamic rate models are indeed predictive. Until then, one would be able to use them only to generate hypothetical concentration curves under a variety of temperature histories and examine the potential consequences. As to the isothermal versions of the models, they can already be used to describe experimental data, generate realistic scenarios, and quantify their implications. Two interactive programs to do that are now part of the Wolfram Demonstrations Project's

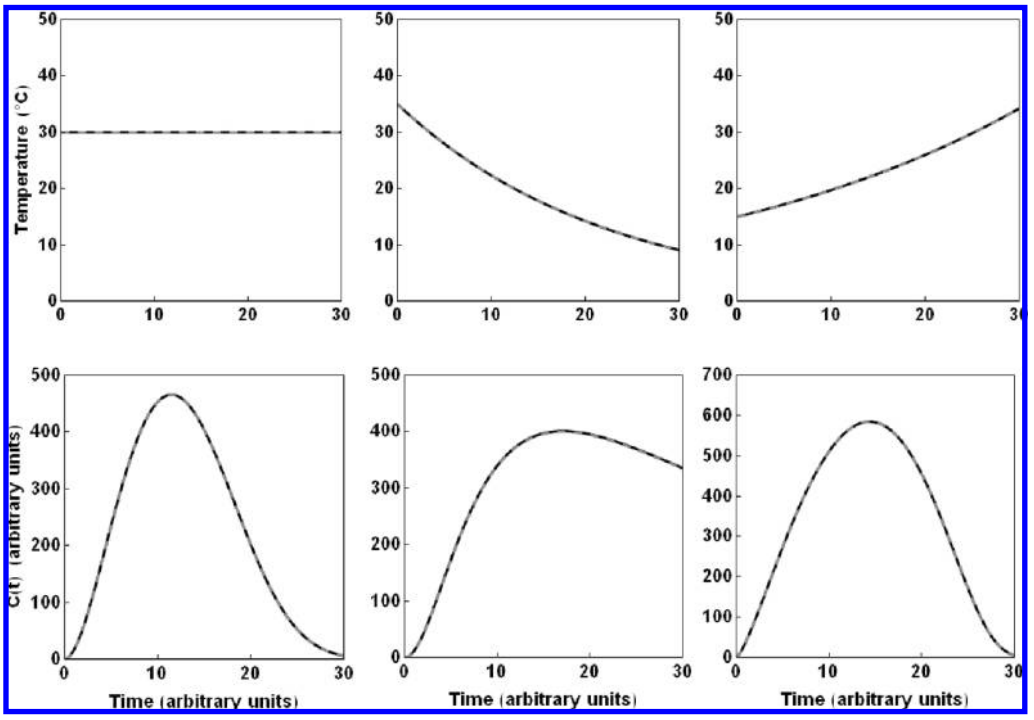

Figure 11. Demonstrations of the internal consistency of eq 15 as a rate model. The solid gray and dashed black curves were generated with the temperature profile being described by different algebraic expressions. Note the almost perfect overlap despite the fact that the concentration curves start at zero and that the boundary conditions had to be estimated using the procedure illustrated schematically in **Figure 8** and explained in the text.

collection. These demonstrations are posted as freeware and can be watched and downloaded at http://demonstrations.wolfram.com/DeNovoGrowthProcessesWithCompetingMechanisms/ and http://demonstrations.wolfram.com/IncipientGrowthProcessesWithCompetingMechanisms/. All the user has to do is set or adjust the model's parameters by moving sliders on the screen and the corresponding $C_g(t)$, $f_d(t)$, and $C(t)$ versus time curves will appear instantaneously.

ACKNOWLEDGMENT

We thank Dr. Benny Davidovitch of the University of Massachusetts Physics Department for a most helpful comment.

LITERATURE CITED

(1) van Boekel, M. A. J. S. *Kinetic Modeling of Reactions in Foods*; CRC Press, Taylor and Francis: Boca Raton, FL, 2009.

(2) Cook, D. J.; Taylor, A. J. On-line MS/MS monitoring of acrylamide generation in potato and cereal-based systems. *J. Agric. Food Chem.* **2005**, *53*, 8926–8933.

(3) Knol, J. J.; Viklund, G. A. I.; Linssen, J. P. H.; Sjoholm, I. M.; Skog, K. I.; van Boekel, M. A. J. S. A study on the use of empirical models to predict the formation of acrylamide in potato crisps. *Mol. Nutr. Food Res.* **2008**, *52*, 313–321.

(4) Rydberg, P.; Eriksson, S.; Tareke, E.; Karlsson, P.; Ehrenberg, L.; Tornqvist, M. Investigations of factors that influence the acrylamide content of heated foodstuffs. *J. Agric. Food Chem.* **2003**, *51*, 7012–7018.

(5) Calligaris, S.; Manzocco, L.; Conte, L. S.; Nicoli, M. C. Application of a modified Arrhenius equation for the evaluation of oxidation rate of sunflower oil at subzero temperatures. *J. Food Sci.* **2004**, *69*, 361–366.

(6) Calligaris, S.; Manzocco, L.; Nicoli, M. C. Modelling the temperature dependence of oxidation rate in water-in-oil emulsions stored at sub-zero temperatures. *Food Chem.* **2007**, *101*, 1019–1024.

(7) Choe, E.; Min, D. B. Mechanism and factors of edible oil oxidation. *Compr. Rev. Food Sci.* **2006**, *5*, 169–186.

(8) Sathivel, S.; Huang, J.; Prinyawiwatkul, W. Thermal properties and applications of the Arrhenius equation for evaluating viscosity and oxidation rates of unrefined pollock oil. *J. Food Eng.* **2008**, *84*, 187–193.

(9) Crapiste, G. H.; Brevedan, M. I. V.; Carelli, A. A. Oxidation of sunflower oil during storage. *J. Agric. Food Chem.* **1999**, *76*, 1437–1443.

(10) Claeys, W. L.; de Vleeschouwer, K.; Hendrickx, M. E. Kinetics of acrylamide formation and elimination during heating of an asparagine−sugar model system. *J. Agric. Food Chem.* **2005**, *53*, 9999–10005.

(11) Halder, A.; Dhall, A.; Datta, A. K. An improved, easily implementable, pourous media based model for deepfat frying. Part I: model development and input parameters. *Food Bioprod. Process.* **2007**, *85*, 209–219.

(12) Peleg, M. *Advanced Quantitative Microbiology for Food and Biosystems: Models for Predicting Growth and Inactivation*; CRC Press: Boca Raton, FL, 2006.

(13) Corradini, M. G.; Normand, M. D.; Peleg, M. Non-linear kinetics: principles and potential food applications. In *Food Engineering: Integrated Approaches*; Gutiérrez-Lopez, G. F., Barbosa-Cánovas, G. V., Welti-Chanes, J., Parada-Arias, E., Eds.; Springer Verlag: New York, 2008; pp 47−72.

(14) Wolever, T. M. S.; Gibbs, A. L.; Spolar, M.; Hitchner, E. V.; Heimowitz, C. Equivalent glycemic load (EGL): a method for quantifying the glycemic responses elicited by low carbohydrate foods. *Nutr. Metab.* **2006**, *3*, 33 (doi:10.1186/1743-7075-3-33).

(15) Parcell, A. C.; Drummond, M. J.; Christopherson, E. D.; Hoyt, G. L.; Cherry, J. A. Glycemic and insulinemic responses to protein supplements. *J. Am. Diet. Assoc.* **2004**, *104*, 1800–1804.

(16) Kallen, A. *Computational Pharmacokinetics*; Chapman and Hall/CRC Biostatistics Series: Boca Raton, FL, 2007.

(17) Baroody, F. M.; Ford, S.; Proud, D.; Kagey-Sobotka, A.; Lichtenstein, L.; Naclerio, R. M. Relationship between histamine and physiological changes during the early response to nasal antigen provocation. *J. Appl. Physiol.* **1999**, *86*, 659–668.

(18) Dougherty, D. P.; Breidt, F.; McFeeters, R. F.; Lubkin, S. R. Energy-based dynamic model for variable temperature batch fermentation by *Lactococcus lactis*. *Appl. Environ. Microbiol.* **2002**, *68*, 2468-2478.

(19) Liu, Y. H.; Bi, J. X.; Zeng, A. P.; Yuan, J. Q. A simple kinetic model for myeloma cell culture with consideration of lysine limitation. *Bioprocess Biosyst. Eng.* **2008**, *31*, 569–577.

(20) Sitton, G.; Srienc, F. Mammalian cell culture scale-up and fed-batch control using automated flow cytometry. *J. Biotechnol.* **2008**, *135*, 174–180.

(21) Aragao, G. M. F.; Corradini, M. G.; Peleg, M. A phenomenological model of the peroxide value's rise and fall during lipids oxidation. *J. Am. Oil Chem. Soc.* **2008**, *85*, 1143–1153.

(22) Corradini, M. G.; Peleg, M. Linear and non-linear kinetics in the synthesis and degradation of acrylamide in foods and model systems. *Crit. Rev. Food Sci.* **2006**, *46*, 489–517.

(23) Peleg, M.; Penchina, C. M. Modeling microbial survival during exposure to a lethal agent with varying intensity. *Crit. Rev. Food Sci.* **2000**, *40*, 159–172.

(24) Corradini, M. G.; Peleg, M. Estimating non-isothermal bacterial growth in foods from isothermal experimental data. *J. Appl. Microbiol.* **2005**, *99*, 187–200.

(25) Corradini, M. G.; Peleg, M. Prediction of vitamin loss during non-isothermal heat processes and storage with non-linear kinetic models. *Trends Food Sci. Technol.* **2006**, *17*, 24–34.

(26) Corradini, M. G.; Peleg, M. Demonstration of the Weibull-Log logistic survival model's applicability to non isothermal inactivation of *E. coli* K12 MG1655. *J. Food Prot.* **2004**, *67*, 2617–2621.

(27) Jiang, B.; Liu, Y.; Bhandari, B.; Zhou, W. Impact of caramelization on the glass transition temperature of several caramelized sugars. Part I: chemical analyses. *J. Agric. Food Chem.* **2008**, *56*, 5138–5147.

(28) Quintas, M.; Guimarães, C.; Baylina, J.; Brandão, T. R. S.; Silva, C. L. M. Multiresponse modelling of the caramelisation reaction. *Innovative Food Sci. Emerging Technol.* **2007**, *8*, 306–315.

Received April 15, 2009. Revised manuscript received July 2, 2009. Accepted July 8, 2009. Contribution of the Massachusetts Agricultural Experiment Station in Amherst.